Vehicles of inverted hexagonal liquid crystalline lipid phases self-assembled at room temperature

B. ANGELOV*, A. ANGELOVA[a], V. M. GARAMUS[B], S. LESIEUR[a]
Inst. of Macromol. Chemistry, Acad. Sci. Czech Rep., Heyrovskeho nam. 2, 16200 Prague, Czech Rep.,
[a]CNRS UMR8612 Institut Galien Paris-Sud, Univ Paris Sud 11, Châtenay-Malabry, France,
[b]Helmholtz-Zentrum Geesthacht, Centre for Materials and Coastal Research, 21502 Geesthacht, Germany

Dispersed nonlamellar lipid phases offer one of the most important contemporary ways for the development of new materials for drug delivery vehicles. The structure of self-assembled vehicles of an inverted hexagonal type liquid crystalline (LC) lipid phase was investigated by means of small angle X-ray scattering (SAXS), quasi-elastic light scattering (QELS), and cross-polarised light optical microscopy (POM). A notable difference was established between the SAXS patterns of the bulk inverted hexagonal (H_{II}) phase and the corresponding nanoparticles (NPs) dispersion. The structure of the hexosome NPs appeared to be more hydrated than that of the bulk H_{II} phase. Both systems were stable at room temperature.

(Received January 29, 2013; accepted April 11, 2013)

Keywords: liquid crystalline lipid nanoparticles, small angle X-ray scattering, cross-polarised light optical microscopy

1. Introduction

Inverted hexagonal (H_{II}) liquid crystalline amphiphilic phases (Figure 1) are being intensively investigated for applications in the design of nanochanneled functional materials, drug and gene delivery systems, diagnostics, structural biology, etc. [1-33]. Particles produced upon the fragmentation and dispersion of H_{II}-phase structures, hexosomes, have been studies as controlled release delivery vehicles [4,24-28]. Hexosome nanoparticles (NPs) have exhibited very high (greater than 95 %) entrapment efficiency for lipophilic drugs as well as penetration enhancing effects [25]. It has been hypothesized that the aqueous and the hydrophobic compartments of the hexosome carriers can provide slower release rates as compared to cubic-phase systems, and hence, may be more effective for sustained release of drugs [4, 5]. However, in a number of lyotropic lipid systems, the nonlamellar H_{II} phase can only be formed at elevated temperatures (> 70 ^{o}C) because heating induces increase in the intrinsic lipid monolayer curvature and anisotropy [13,14]. Therefore, it would be desirable to find out amphiphilic systems and formulation conditions favouring the production of H_{II} phases at room temperature. High resolution structural studies [7,13,14,27,34-38] have contributed to find out lipid compositions and curvature-designer methodologies permitting to suppress the temperature of the nonlamellar cubic-to-H_{II}-phase transition down to ambient and body temperatures.

In this work, a low energy method was employed for the preparation of H_{II}-phase lipid nanovehicles, which stably exist at room temperature. Based on the proposed approach for H_{II}-phase stabilisation at room temperature [7], fine tuning of the lyotropic lipid phase state was performed by self-assembly of hydrated monoglycerides of two different sources.

Dispersions of hexosome NPs were obtained upon incorporation of a PEGylated amphiphile in the lipid system. The liquid crystalline phase identification and structure determination were done by cross-polarized light optical microscopy (POM) and small-angle X-ray scattering (SAXS) methods.

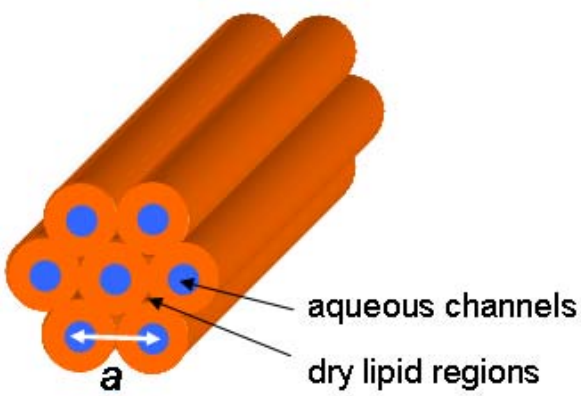

Fig. 1. Anisotropic nonlamellar structural organization of an inverted hexagonal (H_{II}) lyotropic lipid phase.

2. Experimental details

The investigated lipid composition was varies through the ratio (MO/GO) of glycerol monooleates purchased from two different providers. Pure glycerol monooleate

(MO) was in the powder form of 1-monooleoyl-*rac*-glycerol (purity >99.5%, Sigma-Aldrich). The pharmaceutical-grade glycerol monooleate (GO) is an isotropic liquid product and was purchased by the NOF Corporation (NOFABLE GO-991, *Japanese Pharmaceutical Excipient*, ultra-purity oleic acid). GO contains diglycerol monooleate and oleic acid additives [7]. It serves for the manipulation of the bicontinuous cubic-to-H_{II} phase transition temperature of pure MO through its oleic acid additive [7,24]. D-α-tocopherol polyethylene glycol (V_{1000}) was obtained from Sigma-Aldrich and used as a steric stabilizer of the MO/GO vehicles. Liquid crystalline samples were prepared by hydration of a lyophilized mixed lipid film followed by vortex shaking and sonication [19]. For the POM investigations, the lyophilized lipid mixtures were hydrated at lipid/water ratio 50/50 (wt/wt). For preparation of NP dispersion in excess water, the lipid/water ratio was 2/98 (wt/wt). The structures of the samples at lipid contents of 2 wt% (NPs) and 50 wt% (bulk phase) were investigated by SAXS with the purpose of comparison.

2.1 Quasi-Elastic Light Scattering (QELS)

The particle size distributions in the investigated lipid dispersion were determined using a Nanosizer apparatus (Nano-ZS90, MALVERN) equipped with a helium−neon laser of 633 nm wavelength. The following experimental parameters were used: temperature, 25 °C; scattering angle, 90°; refracting index, 1.33; aqueous medium viscosity, 0.890 cP. The results were analyzed using the MALVERN Zetasizer software (version 6.11) and presented as volume statistic distribution plots of the particles hydrodynamic diameters, $d_h = k_B T/3\eta\pi D$, where k_B is the Boltzmann constant, T is temperature, η is the viscosity of the aqueous medium, and D is the mean translational diffusion coefficient of the particles defined by the Stokes−Einstein law for spherical particles in the absence of interactions. The plotted maximal intensities (volume %) correspond to the mean NP sizes, which are most abundant in the sample.

2.2 Polarised Optical Microscopy (POM)

Thin films of LC samples were studied under cross polarizers by POM using cells of two cover glass slides inserted in a temperature-controlled stage. The experimental setup included a microscope Nikon Eclipse E600 equipped with a polariser and a Mightex Buffer USB camera (Mightex Systems). Objectives with magnification of ×20 and ×10 were employed.

2.3 Small-angle X-ray Scattering (SAXS)

SAXS experiments were performed at the P12 BioSAXS beamline of the European Molecular Biology Laboratory (EMBL) at the storage ring PETRA III of the Deutsche Elektronen Synchrotron (DESY, Hamburg, Germany) at 25 °C using a Pilatus 2M detector (1475 x 1679 pixels) (Dectris, Switzerland) and synchrotron radiation with a wavelength λ = 1 Å. The sample-to-detector distance was 3 m. The q-vector was defined as $q = (4\pi/\lambda) \sin\theta$, where 2θ is the scattering angle. The final scattering curves were obtained using the program PRIMUS.

3. Results and discussion

Fig. 2 presents cross-polarized light optical microscope (POM) images of a hydrated self-assembled monoglyceride mixture MO/GO 75/25 (wt/wt). The lipid sample was first heated to 55 °C in order to get a homogeneous thin liquid crystalline layer, the organization of which was examined under cross polarizers as a function of temperature (Fig.2, on cooling; and Figure 3, on heating).

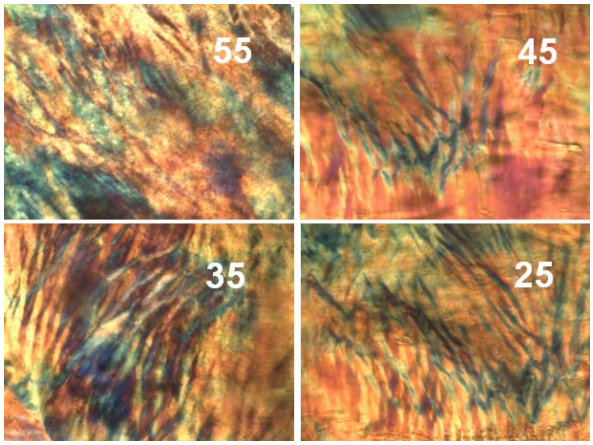

Fig. 2. Cross-polarised optical microscopy images of a bulk MO/GO 75/25 sample, which was heated to 55 °C and step cooled down to 25 °C. (Image sizes: 440 x 330 μm²).

The striation patterns and the angular (fan-shaped) textures in the POM images revealed textures typical for stable inverted hexagonal (H_{II}) phases [12, 26]. The observed birefringence reflected the high anisotropy of the supramolecular liquid crystalline organization resulting from the anisotropic distribution in the lipid monolayer curvature. The cylindrical tubes, formed by the highly curved lipid monolayers in the H_{II}-phase structure (Fig. 1), were found to be packed in domains. Figure 3 shows that the domain size may reach several micrometers.

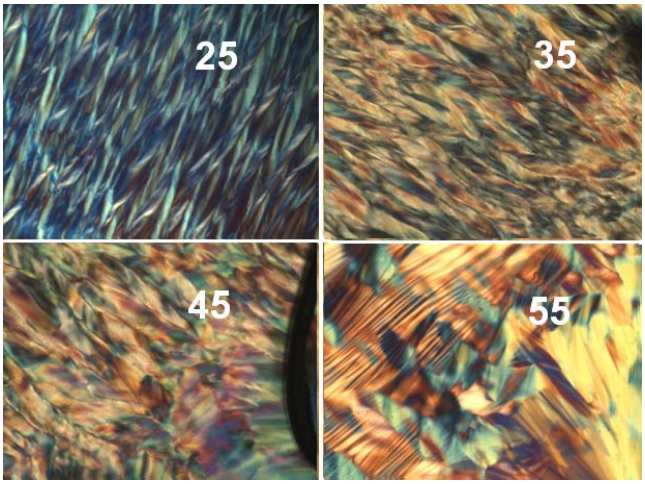

Fig. 3. Cross-polarised optical microscopy images of a bulk MO/GO 75/25 sample, which was conditioned at 25 °C and step heated to 55 °C (Image sizes: 440 x 330 μm^2).

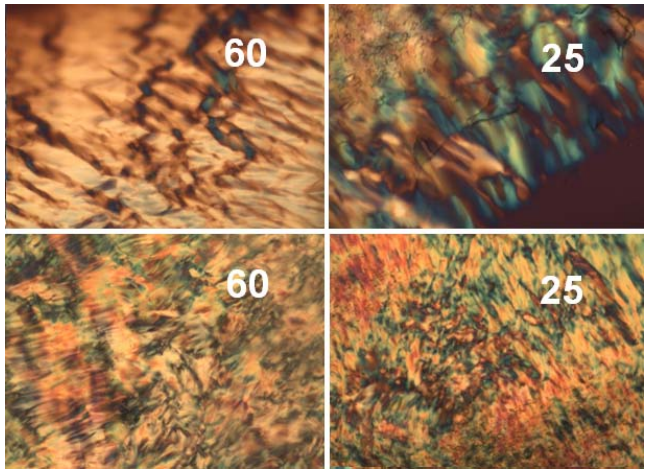

Fig. 4. Cross-polarised optical microscopy images of a bulk MO/GO 70/30 sample. Top panel: sample prepared at 60 °C and imaged at 25 °C (Image sizes: 440 x 330 μm^2); Bottom panel: sample imaged at 60 °C and at 25 °C (Image sizes: 890 x 660 μm^2).

The comparison of the POM images in Figs. 2 and 3 indicated that the sample history and temperature treatment may considerably influence the distribution of domain sizes as well as the domain orientation and alignment. The packing of the cylindrical tubes was better expressed upon step-heating conditioning of the sample (Fig. 3). Rising the temperature favours higher monolayer curvatures and hence better ordering of the H_{II}-phase domains. This result corroborates with previous reports, which have emphasized that the preparation method (for instance ultrasonication, room temperature mechanical dispersion, high-pressure microfluidization, high-temperature autoclaving, or dilution through solvent displacement from amphiphilic mixtures in hydrotropic solvent-ethanol) may be crucial for the resulting domain organization and order in the LC samples [4,24,27].

The POM images of the MO/GO assembly (70/30, wt/wt), used for NPs preparations, are given in Figure 4. The observed anisotropic textures and defect lines are characteristic of an inverted hexagonal LC phase formation [28]. The MO/GO (70/30 wt/wt) mixture was subjected to top-down fragmentation into NPs using 5 mol% of an amphiphilic dispersing agent (V_{1000}) and sonication in an ice bath. In this system, NPs do not form in the absence of V_{1000}, which is necessary for the disruption of the bulk LC domains into submicron entities upon agitation.

Fig. 5 shows the SAXS pattern of the bulk MO/GO system (75/25, wt/wt) self-assembled in excess aqueous buffer phase. The resolved Bragg diffraction peaks maxima, spaced in the ratio of √1 : √3 : √4, undoubtedly confirm the H_{II} phase arrangement of the investigated LC mixture. The lattice parameter of the bulk H_{II} phase, determined from the positions of its (10), (11) and (20) reflections, is a_h = 5.8 nm. It characterizes the periodicity of the structure (Figure 1) consisting of bundles of inverted cylinders of lipid molecules surrounding infinitely long aqueous channels that are packed on a two-dimensional hexagonal lattice.

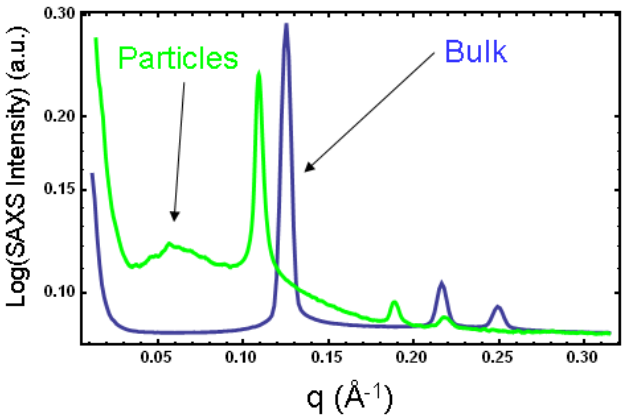

Fig 5. SAXS patterns of a bulk LC sample (blue plot) and of dispersed nanoparticles stabilized by V_{1000} (green curve). The Bragg peaks are spaced in the ratio of √1 : √3 : √4. The peak at q ~ 0.06 Å^{-1} corresponds to the form factor component of the NPs scattering.

The inner organization of the dispersed lipid NPs (2 wt% lipid) was also found to be of an inverted hexagonal (H_{II}) type structure as the parent bulk phase (50 wt% lipid). Therefore, the employed non-ionic PEGylated amphiphile, D-α-tocopherol polyethylene glycol (V_{1000}), appears to be an efficient hydrophilic stabilizer of the NPs with a H_{II}-phase structure. The NPs stabilization at room temperature is provided by the created PEG-shell surrounding the particles. A lattice parameter, a_h = 6.64 nm, was determined from the SAXS pattern in Figure 5 (green curve). The comparison of the lattice parameters of the dispersed and the non-dispersed lipid samples (Fig. 5) revealed that the structure of the hexosome NPs appears to be more hydrated than that of the bulk H_{II} phase. This result is essential for the sustained release properties of the investigated nanostructures.

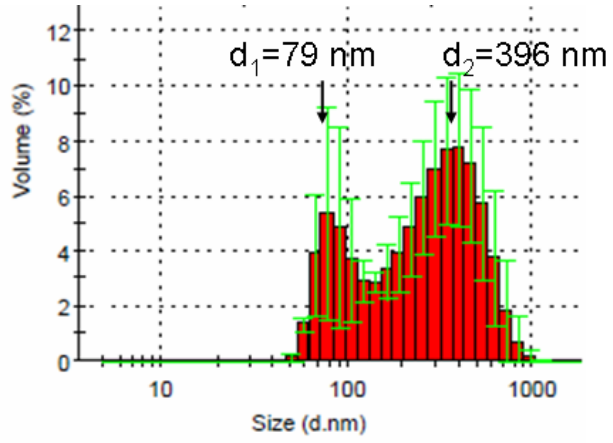

Fig. 6. NPs size distribution, determined by QELS at 25 °C, for a MO/GO 70/30 sample dispersed in the presence of 5 mol% of D-α-tocopherol polyethylene glycol (V_{1000}).

The sizes of the obtained sterically stabilized lipid particles in the milky white dispersion were determined by quasi-elastic light scattering (QELS). Figure 6 shows the volume distribution of the hexosome particle dimensions. It reveals two mean sizes of the NPs of around 80 nm and 400 nm, respectively. In individual state, the amphiphile V_{1000} forms micelles with a hydrodynamic diameter of ~10 nm. The absence of a micellar population in Fig. 6 implies that V_{1000} is incorporated in the lipid NPs.

4. Conclusion

Stable hexosome nanovehicles were obtained at room temperature using a monoglyceride lipid mixture of pharmaceutical interest. Studies are in progress to evaluate the interaction of the prepared NPs with guest biomolecules.

Acknowledgements

This paper contains results presented at the International Summer School and Workshop "Complex and Magnetic Soft Matter Systems: Physico-Mechanical Properties and Structure", CMSMS 12, 3-7 September 2012, Alushta, Ukraine (http://cmsms.jinr.ru/). B.A. acknowledges the Czech Science Foundation Grant No. P208/10/1600. J.-J. Vachon and F. Khidache are acknowledged for assistance with the optical microscope set up. A.A. and S.L. acknowledge supports from ANR SIMI10 Nanosciences and LabEx LERMIT.

References

[1] I. W. Hamley, Soft Matter **6**, 1863 (2010).
[2] S. Manet, J. Schmitt, M. Impéror-Clerc, V. Zholobenko, D. Durand, C.L.P. Oliveira, J.S. Pedersen, C. Gervais, N. Baccile, F. Babonneau, I. Grillo, F. Meneau, C. Rochas, J. Phys. Chem. B **115**, 11330 (2011).
[3] I. Petrov, A. Angelova, Langmuir, **8**, 3109 (1992).
[4] B. J. Boyd, S. B. Rizwan, Y-D. Dong, S. Hook, T. Rades, Langmuir **23**, 12461 (2007).
[5] S. Phan, W-K. Fong, N. Kirby, T. Hanley, B. J. Boyd, Int. J. Pharm. **421**, 176 (2011).
[6] A. Angelova, B. Angelov, V.M. Garamus, P. Couvreur, S. Lesieur, J. Phys. Chem. Lett. **3**, 445 (2012).
[7] B. Angelov, A. Angelova, R. Mutafchieva, S. Lesieur, U. Vainio, V.M. Garamus, G.V. Jensen, J.S. Pedersen, Phys. Chem. Chem. Phys. **13**, 3073 (2011).
[8] A. Angelova, B. Angelov, B. Papahadjopoulos-Sternberg, M. Ollivon, C. Bourgaux, J. Drug Deliv. Sci. Technol. **15**, 108 (2005).
[9] N. I. Zahid, O. K. Abou-Zied, R. Hashim, T. Heidelberg, Langmuir **28**, 4989 (2012).
[10] B. Angelov, M. Ollivon, A. Angelova, Langmuir **15**, 8225 (1999).
[11] S. Andersson, M. Jacob, S. Lidin, K. Larsson, Z. Kristallogr. **210**, 315 (1994).
[12] L. Ramos, P. Fabre, Langmuir **13**, 682 (1997).
[13] T. Mareš, M. Daniel, S. Perutkova, A. Perne, G. Dolinar, A. Iglič, M. Rappolt, Kralj-Iglič, J. Phys. Chem. B **112**, 16575 (2008).
[14] A. Angelova, M. Ollivon, A. Campitelli, C. Bourgaux, Langmuir **19**, 6928 (2003).
[15] G. E. Schröder-Turk, T. Varslot, L. de Campo, S. C. Kapfer, W. Mickel, Langmuir **27**, 10475 (2011).
[16] I. Amar-Yuli, J. Adamcik, S. Blau, A. Aserin, N. Garti, R. Mezzenga, Soft Matter **7**, 8162 (2011).
[17] Zabara, I. Amar-Yuli, R. Mezzenga, Langmuir **27**, 6418 (2011).

[18] B. Angelov, A. Angelova, B. Papahadjopoulos-Sternberg, S. Lesieur, J-F. Sadoc, M. Ollivon, P. Couvreur, J. Am. Chem. Soc. **128**, 5813 (2006).
[19] B. Angelov, A. Angelova, S. Filippov, G. Karlsson, N. Terrill, S. Lesieur, P. Štěpánek, Soft Matter. **7**, 9714 (2011).
[20] B. Angelov, A. Angelova, B. Papahadjopoulos-Sternberg, S. V. Hoffmann, V. Nicolas, S. Lesieur, J. Phys. Chem. B **116**, 7676 (2012).
[21] A. Angelova, B. Angelov, B. Papahadjopoulos-Sternberg, C. Bourgaux, P. Couvreur, J. Phys. Chem. B, **109**, 3089 (2005).
[22] C. Nilsson, K. Edwards, J. Eriksson, S.W. Larsen, J. Østergaard, C. Larsen, A. Urtti, A. Yaghmur, Langmuir **28**, 11755 (2012).
[23] A. Yaghmur, L. Paasonen, M. Yliperttula, A. Urtti, M. Rappolt, J. Phys. Chem. Lett. **1**, 962 (2010).
[24] M. Nakano, T. Teshigawara, A. Sugita, W. Leesajakul, A. Taniguchi, T. Kamo, H. Matsuoka, T. Handa, Langmuir **18**, 9283 (2002).
[25] N.K. Swarnakar,V. Jain, V. Dubey, D. Mishra, N.K. Jain, Pharm Res. **24**, 2223 (2007).
[26] B.J. Boyd, D. V. Whittaker, S-M. Khoo, G. Davey, Int. J. Pharm. **318**, 154 (2006).
[27] Y-D. Dong, I. Larson, T. Hanley, B.J. Boyd, B.J. Langmuir **22**, 9512 (2006).
[28] F.C. Rossetti, M.C.A. Fantini, A.R.H. Carollo, A.C. Tedesco, M.V.L.B. Bentley, Pharm. Sci. **100**, 2849 (2011).
[29] T-H. Nguyen, T. Hanley, C.J.H. Porter, B.J. Boyd, Drug. Deliv. Transl. Res. **1**, 429 (2011).
[30] M. Rosa, M.R. Infante, M.G. Miguel, B. Lindman, Langmuir **22**, 5588 (2006).
[31] S. Guillot, C. Moitzi, S. Salentinig, L. Sagalowicz, M.E. Leser, O. Glatter, Colloids Surf. A - Physicochem. Eng. Aspects **291**, 78 (2006).
[32] S. Guillot, S. Salentinig, A. Chemelli, L. Sagalowicz, M.E. Leser, O. Glatter, Langmuir **26**, 6222 (2010).
[33] C. Fong, A. Weerawardena, S.M. Sagnella, X. Mullet, L. Waddington, I. Krodkiewska, C.J. Drummond, Soft Matter **6**, 4727 (2010).
[34] B. Angelov, A. Angelova, V. M. Garamus, M. Drechsler, R. Willumeit, R. Mutafchieva, P. Štěpánek, S. Lesieur, Langmuir, **28**, 16647 (2012).
[35] A. Angelova, J.G. Petrov, T. Dudev, B. Galabov, Colloids and Surfaces, **60**, 351 (1991).
[36] B. Angelov, A. Angelova, U. Vainio, V. M. Garamus, S. Lesieur, R. Willumeit, P. Couvreur, Langmuir, **25**, 3734 (2009).
[37] A. Angelova, B. Angelov, S. Lesieur, R. Mutafchieva, M. Ollivon, C. Bourgaux, R. Willumeit, P. Couvreur, J. Drug Deliv. Sci. Technol. **18**, 41 (2008).
[38] B. Angelov, A. Angelova, M. Ollivon, C. Bourgaux, A. Campitelli, J. Am. Chem. Soc. **125**, 7188 (2003).

*Corresponding author: angelov@imc.cas.cz